Diiron bis-cyclopentadienyl complexes as transfer hydrogenation catalysts: The key role of the bridging aminocarbyne ligand

Diiron Bis-Cyclopentadienyl Complexes as Transfer Hydrogenation Catalysts: The Key Role of the Bridging Aminocarbyne Ligand

Giulio Bresciani,[a,c] Lorenzo Biancalana,[a,c] Stefano Zacchini,[b,c] Guido Pampaloni,[a,c] Gianluca Ciancaleoni,[a,c,*] Fabio Marchetti[a,c,*]

[a] University of Pisa, Department of Chemistry and Industrial Chemistry, Via G. Moruzzi 13, I-56124 Pisa, Italy.

[b] University of Bologna, Department of Industrial Chemistry "Toso Montanari", Viale Risorgimento 4, I-40136 Bologna, Italy.

[c] CIRCC, Via Celso Ulpiani 27, I-70126 Bari, Italy.

Corresponding Authors

*E-mail addresses: gianluca.ciancaleoni@unipi.it; fabio.marchetti@unipi.it

Webpage: https://people.unipi.it/fabio_marchetti/

Abstract

The catalytic activity of a series of diiron complexes based on the $\{Fe_2Cp_2(CO)_x\}$ core (x = 2-3) and containing a bridging aminocarbyne ligand was screened in transfer hydrogenation reaction of cyclohexanone from isopropanol. The series include cationic tricarbonyl complexes, **[1a-d]CF_3SO_3**, and neutral derivatives obtained by substitution of one carbonyl with hydride (**2a-c**), cyanide (**3a-d**) or chloride (**4a**) ligands. The novel compounds **2a-b**, **3a-b** and **4a** were characterized by analytical and spectroscopic techniques, and the single crystal X-ray structure of one isomer of **4a** was determined. In general, diiron complexes exhibited a moderate activity in combination with potassium hydroxide; $[Fe_2Cp_2(CN)(CO)(\mu\text{-}CO)\{\mu\text{-}CN(Me)(4\text{-}C_6H_4OMe)\}]$, **3a**, emerged as the best catalyst and the study of its activity was extended to a range of other ketones. DFT calculations suggest an unusual carbyne-centred mechanism, and the better performance displayed by **3a** is ascribable to the stabilizing effect provided by the cyanide co-ligand, which is experimentally supported by IR analyses.

Keywords: transfer hydrogenation; diiron complexes; aminocarbyne ligand; DFT calculations; cyano group.

Introduction

The reduction of carbonyls, imines and other unsaturated organic functions into the corresponding hydrogenated derivatives is a key industrial reaction to produce fine chemicals, and transfer hydrogenation (TH) from suitable substrates has attracted huge interest since it represents a valid alternative to the use of dihydrogen gas.[1,2] The development of outstanding ruthenium catalysts for asymmetric hydrogenation eventually led to the assignment of the Nobel Prize to Noyori in 2001.[3,4] In general, the catalytic cycle during the TH process starts with the formation of ruthenium-hydride complexes, then hydride transfer to the unsaturated organic substrate may sometimes occur in a concerted way assisted by a protic function on another ligand.[5,6,7] Similar mechanistic pathways have been accepted and proposed for a wide variety of heterometallic complexes.[8,9,10] Homogeneous

catalysts for TH reaction are usually based on second and third row transition metals, however the ultimate demand for sustainability has fueled the search for more environmentally benign and cost-effective metal systems.[11,12,13,14,15,16,17] Iron is ideal as a metal element, since it is abundant, relatively nontoxic in many forms and displays a range of oxidation states.[18,19,20] In this setting, diverse iron compounds have been investigated for TH in the last decade.[11c,21,22,23] These generally possess a mononuclear structure and, among them, a number of piano-stool complexes with a (substituted) cyclopentadienyl ligand has been studied for the ability to promote TH of ketones from isopropanol.[24,25,26,27,28,29] In several cases, the proposed catalytic mechanism resembles that one typical of Noyori-type catalysts, proceeding via the formation of iron-hydride intermediates.[21,30,31,32] Diiron complexes remain undeveloped in the field of TH, and this is somewhat surprising considering that, in general, a bimetallic core may benefit of cooperative effects arising from the two adjacent metal centres, thus enabling on the bridging ligand(s) reactivity patterns otherwise not available in monometallic species.[33,34] Concerning diiron complexes, the metal-metal cooperativity has found practical application in homogeneous catalysis, especially on the way to mimic related enzymatic systems,[35,36] and for the design and the synthesis of a plethora of organometallic structures.[37,38] Diiron tris-carbonyl derivatives containing a bridging aminocarbyne ligand[39] are accessible from the commercially available dimer $[Fe_2Cp_2(CO)_4]$ ($Cp = \eta^5\text{-}C_5H_5$) by a straightforward two-step synthesis working up to multigram scale (Scheme 1).[40] These compounds display a rich and versatile chemistry ranging from CO substitution reactions, addition of nucleophiles and coupling of the aminocarbyne carbon with a variety of unsaturated organic reactants.[38,41] The dinuclear structure is essential to provide stability to the strongly electron-withdrawing aminocarbyne group,[42] allowing at the same time some variability in the type of N-substituents and co-ligands. Only two examples of crystallographically characterized monoiron aminocarbyne complexes have been reported to date.[38,43] Herein, we report a preliminary study focused on the evaluation of the potential of a series of diiron aminocarbyne complexes in TH of simple ketones from isopropanol. We evidence an uncommon mechanism centered on the bridging carbyne.

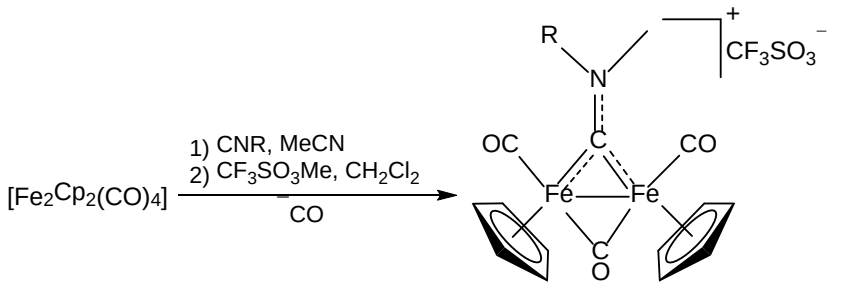

Scheme 1. Synthesis in two steps of diiron cationic μ-aminocarbyne complexes from $[Fe_2Cp_2(CO)_4]$ (R = alkyl, aryl).

Results and discussion

Synthesis and characterization of complexes

The diiron aminocarbyne complexes $[Fe_2Cp_2(CO)_2(\mu\text{-}CO)\{\mu\text{-}CNMe(R)\}]CF_3SO_3$ (R = 4-C_6H_4OMe, **[1a]CF_3SO_3**; R = Cy = C_6H_{11}, **[1b]CF_3SO_3**; R = Xyl = 2,6-$C_6H_3Me_2$, **[1c]CF_3SO_3**; R = CH_2=$CHCH_2$, **[1d]CF_3SO_3**) were synthesized according to published procedures (Scheme 2).[40,44]

Starting from **[1a-d]CF_3SO_3**, we prepared some targeted derivatives by introducing structural modifications which could favour the catalytic TH process. Specifically, complexes with a bridging hydride ligand (**2a-c**) were taken in consideration because metal-hydride species are expected to be important during TH catalytic cycles (see Introduction).[11c,45,46] Complexes **3a-d**, bearing a terminal cyanide ligand, resemble a similar compound (**3e**, R = Me, vide infra) that recently emerged as an efficient catalyst for the electrocatalytic H_2 production from acetic acid, involving the cyanide and carbyne ligands as active centres.[47,48] We reasoned that the chloride ligand in **4a** could be dissociated under suitable conditions, and the subsequent availability of one metal site may favour the catalytic reaction.

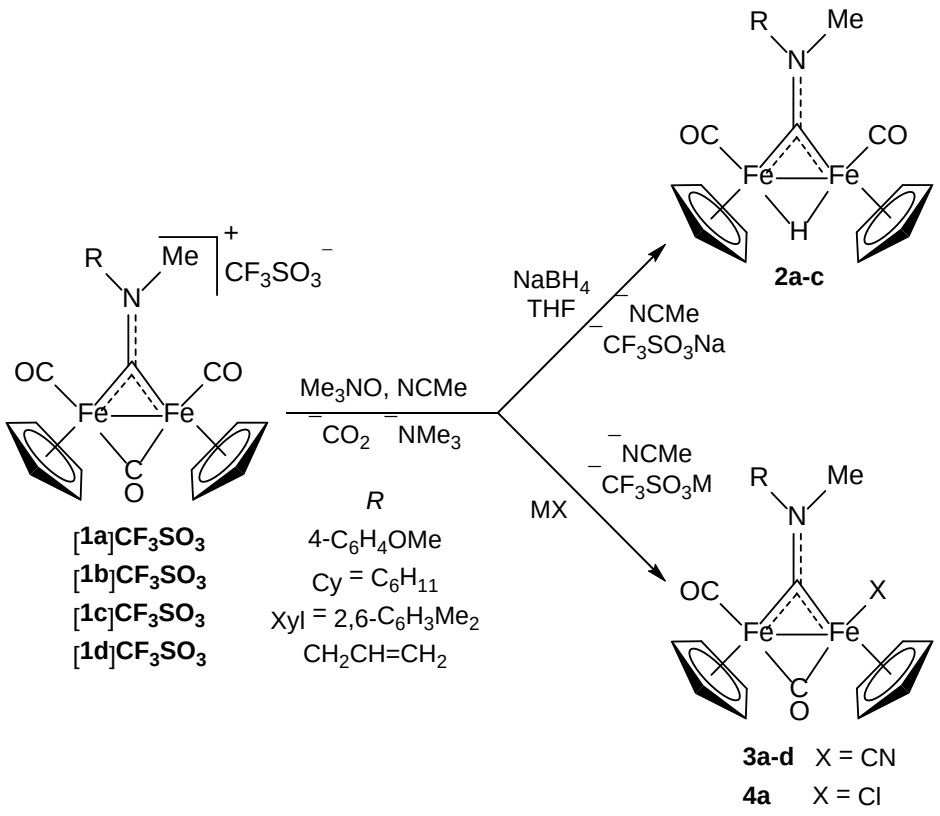

Scheme 2. Synthetic routes to diiron complexes investigated in the present work. MX = NBu_4CN (reaction solvent: CH_2Cl_2) or LiCl (reaction solvent: THF).

The common feature in the synthesis of **2-4** is the elimination of one carbon monoxide ligand by means of the TMNO (trimethylamine-N-oxide) strategy.[49] Thus, when the reaction with TMNO is conducted in acetonitrile, a labile nitrile adduct is formed,[50] and the subsequent treatment with either $NaBH_4$, NBu_4CN or LiCl results in the formation of neutral products. Within the **2a-c** series, $[Fe_2(\mu\text{-}H)Cp_2(CO)_2\{\mu\text{-}CN(Me)(Xyl)\}]$, **2c**, was previously reported,[51] whereas $[Fe_2(\mu\text{-}H)Cp_2(CO)_2\{\mu\text{-}CN(Me)(R)\}]$ (R = 4-C_6H_4OMe, **2a**; R = Cy, **2b**) are described here for the first time. Notably, while **2c** is fairly stable in solution and also as a solid, **2a-b** are much more reactive species (especially in solution): they do not tolerate alumina chromatography and, in chlorinated solvents, they undergo slow hydride-chloride substitution.[52,53] The different behaviour of **2a-b** with respect to **2c** appears correlated with the more pronounced electron donor ability of the aminocarbyne R substituent in the former, enhancing the anionic character of the hydride ligand. On account of their poor stability, **2a-b** could not be fully characterized and were excluded from the catalytic tests. However, the IR spectra of **2a-b** (in acetonitrile solution) match the IR spectrum of **2c**, showing two absorptions related to the terminal carbonyl

ligands (e.g. at 1933 and 1890 cm^{-1} in the case of **2b**). Evidence for the hydride ligand was obtained by ^{1}H NMR spectra, which displayed one signal at around −18 ppm. Complexes **3c-d** are already known,[51,54] whereas **3a-b** were synthesized for the first time; they were purified by alumina chromatography and finally isolated as green solids in ca. 70% yields. Complexes like **3a-b**, of general formula $[Fe_2Cp_2(L)(CO)(\mu\text{-}CO)\{\mu\text{-}CN(Me)(R)\}]$ ($R \neq Me$, L = anionic ligand), may exist in up to four isomeric forms (Figure 1), i.e. cis-trans isomers (referred to the relative orientation of the Cp ligands with respect to the Fe-Fe axis) and α-β isomers (referred to the R and L groups). The latter source of isomerism arises from the fact that the carbyne-nitrogen bond possesses a significant iminium character, thus preventing rotation around the C-N axis and interchange between the Me and R substituents.[38,40]

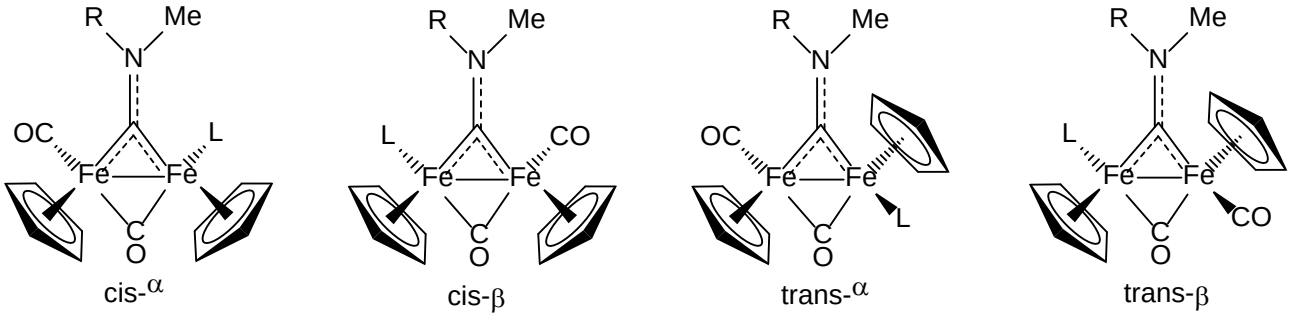

Figure 1. Possible isomers in diiron μ-aminocarbyne derivatives ($R \neq Me$, L = anionic ligand).

The IR spectrum of **3a** (in dichloromethane solution) exhibits an absorption for the cyano group at 2091 cm^{-1}, and three carbonyl bands attributable to cis (1979, 1804 cm^{-1}) and trans isomers (1963, 1804 cm^{-1}), in analogy with data available for related complexes. The IR spectrum of **3b** consists of four main absorptions at 2091, 1978, 1801 and 1560 cm^{-1}, related to the cyanide ligand, the terminal and bridging carbonyl ligands, and the carbyne-nitrogen bond, respectively. Accordingly, the NMR spectra of **3a** (in $CDCl_3$) contain four sets of resonances (cis-α, cis-β, trans-β and trans-α isomers), whereas the NMR spectra of **3b** contain only two sets (cis-α and cis-β isomers). However, NMR signals due to each isomer could not be unambiguously assigned. Salient ^{13}C NMR features are given by the resonance of the aminocarbyne carbon, which falls at typical low-fields (327.6 – 335.9 ppm),[38,55,56,57] and the resonance due to the cyano moiety, occurring at about 120 ppm.

The identity of **3a-b** was further corroborated by ESI-MS spectra, showing the peak due to the molecular cation.

Complex **4a** was obtained in 72% yield, and overall spectroscopic data suggest that this compound is present in solution as a mixture of cis-α and cis-β isomers. The solution IR spectrum exhibits two carbonyl bands at 1979 and 1800 cm^{-1}, and the NMR spectra contain two groups of resonances in a ratio of 2:1, with the aminocarbyne carbon resonating at 342.7 and 342.6 ppm, respectively, in the two isomers. The ESI-MS spectrum of **4a** does not display the peak related to the molecular cation, but a signal related to $[M - Cl]^+$ was clearly recognized, suggesting the lability of the chloride ligand in line with the mechanistic studies (vide infra).

The structure of cis-β-**4a** was ascertained by a single crystal X-ray diffraction study (Figure 2 and Table 1), while we previously reported the X-ray structure of cis-α-**4a**. The C(3)-N(1) bond [1.273(10) Å] possesses some double bond character, as routinely found in related diiron μ-aminocarbyne complexes.[38,40,55]

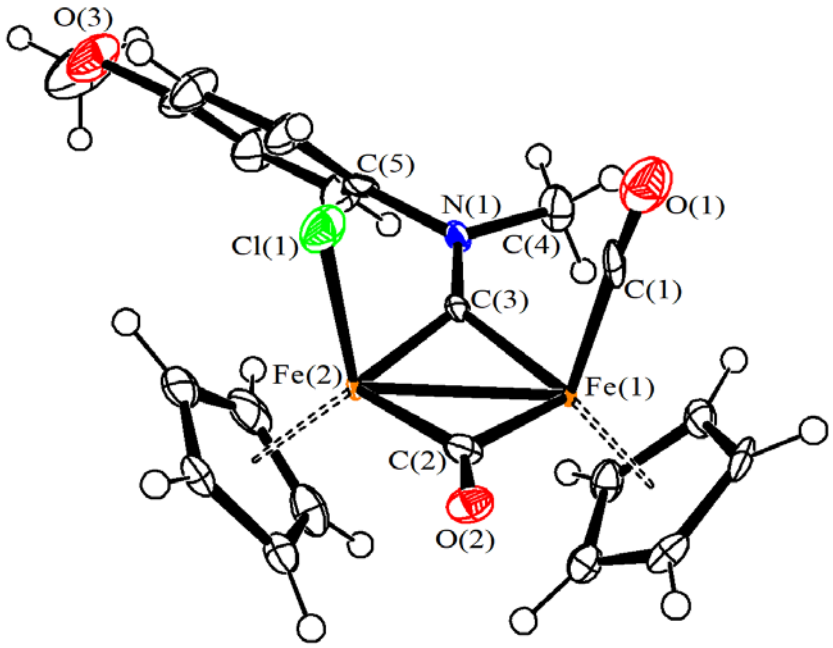

Figure 2. View of the molecular structure of cis-β-**4a**. Displacement ellipsoids are at the 50% probability level.

Table 1. Main bond distances (Å) and angles (°) of cis-β-**4a**.

Fe(1)-Fe(2)	2.4924(14)	Fe(2)-Cl(1)	2.336(2)
Fe(1)-C(2)	1.941(8)	Fe(2)-C(2)	1.874(8)
Fe(1)-C(3)	1.888(7)	Fe(2)-C(3)	1.857(7)

Fe(1)-C(1)	1.814(9)	N(1)-C(3)	1.273(10)
N(1)-C(4)	1.491(10)	N(1)-C(5)	1.453(7)
C(1)-O(1)	1.032(11)	C(2)-O(2)	1.195(9)
Fe(1)-C(1)-O(1)	176.7(8)	Fe(1)-C(2)-Fe(2)	81.6(3)
Fe(1)-C(3)-Fe(2)	83.5(3)	C(3)-N(1)-C(4)	121.6(6)
C(3)-N(1)-C(5)	123.1(6)	C(4)-N(1)-C(5)	115.2(6)

Catalytic studies

We selected cyclohexanone as a model ketone to screen the ability of the diiron complexes to promote the hydrogenation from isopropanol. Potassium hydroxide was employed as the base, in analogy to literature methods.[58,59,60,61,62]

Results were encouraging, and cyclohexanol was afforded in almost quantitative yield after heating at 85 °C for 20 h (Table 2); shortening the reaction time to 8 h led to yields >75% with the cyano-complexes **3a-d**, and especially **3a** revealed efficient (yield = 87%). A blank experiment using only KOH was performed under the same reaction conditions, and confirmed the needing of the metal catalyst to reach satisfactory yields.

Cat. (mol %)	Yield (%)[a]	Time (h)	TON [b]	TOF (h^{-1})[c]
---	30	20	---	---
[1a]CF_3SO_3	98	20	195	9.8
[1a]CF_3SO_3	62	8	124	15.5
[1b]CF_3SO_3	94	20	188	9.4
[1b]CF_3SO_3	55	8	111	13.8
[1c]CF_3SO_3	99	20	198	9.9
[1c]CF_3SO_3	71	8	143	17.9
[1d]CF_3SO_3	96	20	192	9.6
[1d]CF_3SO_3	41	8	82	10.3
2a	98	20	195	9.8
2a	61	8	122	15.2
2c	98	20	195	9.8
2c	53	8	107	13.4
3a	99	20	198	9.9
3a	87	8	173	21.7
3b	99	20	198	9.9
3b	77	8	153	19.2
3c	99	20	198	9.9
3c	92	15	185	12.3
3c	78	8	156	19.4
3d	99	20	198	9.9
3d	83	8	167	20.8
4a	99	20	198	9.9
4a	45	8	91	11.3

Reaction conditions: Cyclohexanone (0.100 mL, 0.968 mmol), catalyst 0.5 mol%, KOH 50 mol%, ^{i}PrOH 2 mL, T = 85 °C. [a]Determined by ^{1}H NMR spectroscopy. [b](number of moles of ketone consumed)/(mole of catalyst). [c]TON/time.

Table 2. Screening of diiron aminocarbyne complexes as catalysts for TH reaction of cyclohexanone from isopropanol.

Based on the preliminary results, compound **3a** was selected for further optimization, thus different bases were tested in variable amounts, and also the amount of catalyst was screened. According to the outcomes reported in Table 3, the most favourable reaction conditions imply the use of **3a** and KOH at the respective concentrations of 0.5 mol% and 50 mol%.

Cat. (mol %)	Yield (%)[a]	Base (mol %)	TON[b]	TOF (h^{-1})[c]
3a (0.5)	87	KOH (50)	173	21.7
3a (0.5)	55	KOH (25)	109	13.6
3a (0.5)	28	KOH (10)	55	6.9
3a (1)	80	KOH (50)	80	10.0
3a (1)	56	KOH (25)	56	6.9
3a (1)	21	KOH (10)	21	2.6
3a (0.5)	67	NaOH (50)	133	16.7
3a (0.5)	73	^{t}BuOK (50)	146	18.2
3a (0.5)	0	0	0	0

Reaction conditions: Cyclohexanone (0.100 mL, 0.968 mmol), ^{i}PrOH 2 mL, T = 85 °C, time = 8 h. [a]Determined by ^{1}H NMR spectroscopy. [b](number of moles of ketone consumed)/(mole of catalyst). [c]TON/time.

Table 3. Optimization of catalyst and base for TH of cyclohexanone from isopropanol.

The optimized reaction parameters were fixed to extend the investigation to a panel of ketones, i.e. acetophenone, 3',4'-dichloroacetophenone, benzophenone, 4-bromobenzophenone, 4-methoxybenzophenone and fluorenone (Table 4). In combination with KOH, **3a** was able to convert most of the investigated ketones into the corresponding alcohols, with variable yields (25-99%). Extending the reaction time to 48 h led a significant increase of the yield only from acetophenone. In general, the catalytic activity displayed by **3a** in TH reaction is lower than what previously reported in the literature for other iron complexes.[21,31]

Substrate	Product	Yield (%)[a]	Time (h)	TON[b]	TOF

					$(h^{-1})^{[c]}$
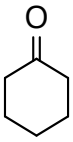	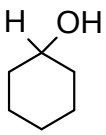	87	8	173	21.7
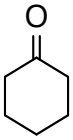	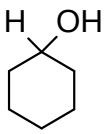	99	20	198	9.9
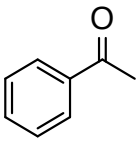	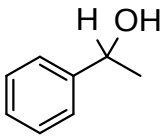	30	8	60	7.5
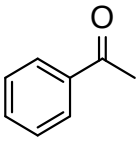	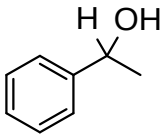	56	20	111	5.6
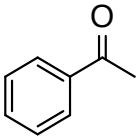	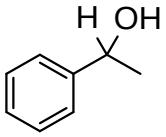	96	48	192	4.0
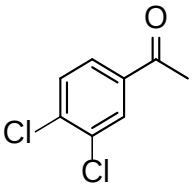	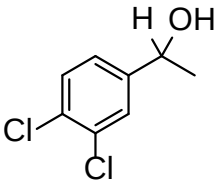	64	20	129	6.4
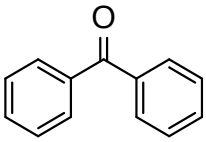	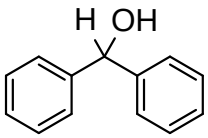	51[d]	8	102	12.8
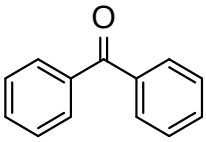	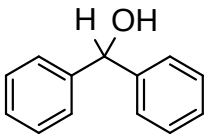	81[d]	20	162	8.1
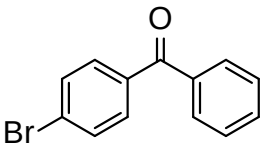	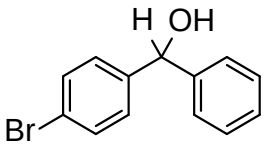	52[d]	8	105	13.1
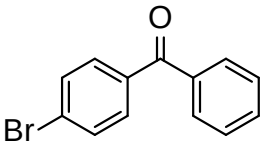	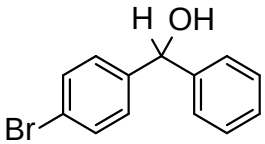	76[d]	20	152	7.6

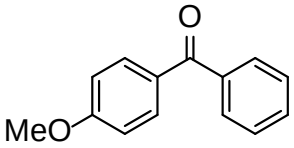	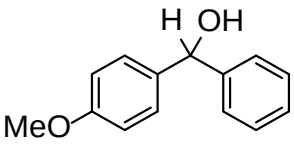	31[d]	20	61	3.1
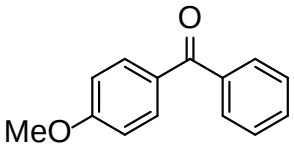	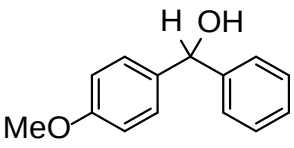	44[d]	48	87	1.8
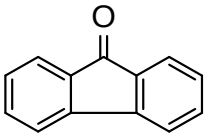	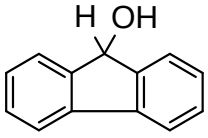	25[d]	20	51	2.5
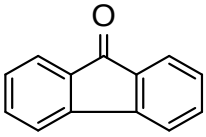	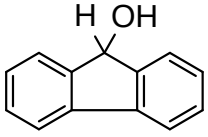	36[d]	48	72	1.5

Reaction conditions: ketone (ca. 1 mmol), ^{i}PrOH 2 mL, KOH (50 mol%), catalyst **3a** (0.5 mol%), T = 85 °C. [a]Determined by ^{1}H NMR spectroscopy. [b](number of moles of ketone consumed)/(mole of catalyst). [c]TON/time. [d]^{1}H NMR spectra recorded in acetone-d_6.

Table 4. TH reaction of different ketones using complex **3a** as catalyst under optimized experimental conditions.

In order to gain information about the mechanism of the different classes of compounds, the stability of **[1a]CF$_3$SO$_3$**, **3a** and **4a**, in isopropanol solution at reflux in the presence of three equivalents of KOH, was monitored by infrared spectroscopy. In the case of **3a**, the spectrum after 2 h pointed to the disappearance of the band at 1978 cm^{-1} and the increase of the intensity of the band at 1963 cm^{-1}, suggesting an almost quantitative conversion of **cis-3a** to **trans-3a** (Figure S15). This outcome agrees with previous considerations by other authors on the higher stability of the related complex *trans*-[Fe_2Cp_2(CN)(CO)(μ-CO){μ-$CNMe_2$}], **trans-3e**, with respect to *cis*-[Fe_2Cp_2(CN)(CO)(μ-CO){μ-$CNMe_2$}], **cis-3e**. Complexes [**1a**]**CF$_3$SO$_3$** and **4a** were almost completely consumed after 1 hour in ^{i}PrOH/KOH at reflux, affording the hydride compound **2a** as the main product and other carbonyl species presumably derived from the decomposition of **2a** (Figures S14 and S16). The formation of **2a** was confirmed by ^{1}H NMR spectroscopy (see Experimental for details). Extensive decomposition was detected after 10 h of thermal treatment of [**1a**]**CF$_3$SO$_3$** and **4a**, however chloride transfer from **4a** to the organic substrate should be excluded.[63,64]

Overall, results highlight the superior stability of the cyanide complex **3a** under the experimental conditions employed in catalysis, therefore **3a** is assumed to behave as the active species in the TH reaction.

Carbonyl-hydride substitution, as observed for [**2a-d**]$^+$, is a well known reaction in organometallic chemistry, proceeding in a basic environment through CO_2 elimination.[65.66] Notwithstanding, formation of bridging hydride from **4a** appears to be the result of chloride displacement and direct hydride transfer from the isopropoxide anion (generated by isopropanol deprotonation) to the iron centre. DFT calculations indicate that the hydride transfer from the isopropoxide anion to the model 34-electrons diiron complex cis-[$Fe_2Cp_2(CO)(\mu\text{-}CO)\{\mu\text{-}CNMe_2\}$]$^+$, bearing a coordination vacancy, to give **cis-2e** and acetone is strongly favoured (-49.8 kcal/mol); a suitable transition state was not found, which suggests a barrierless process. Instead, an alternative pathway to hydride complexes via isopropoxide coordination[67,68] seems unlikely due to the fact that the iron coordination sphere in these systems is too congested to allow β-hydrogen abstraction.

DFT calculations

A DFT study was executed to give hints into the mechanism of the TH reaction promoted by diiron aminocarbyne complexes containing a cyanide or a hydride ligand. Complex [$Fe_2Cp_2(CN)(CO)(\mu\text{-}CO)\{\mu\text{-}CNMe_2\}$], **3e**, was selected as a representative model of the cyanide derivatives **3a-d**. First, the relative stability of possible isomers was calculated. Thus, the trans isomer, **trans-3e**, was found to be more stable than the cis one, **cis-3e**, by 2.5 kcal/mol (Figure 3), in agreement with previous theoretical findings and the experimental evidence from the thermal treatment of **3a** (see above). The terminal coordination of the aminocarbyne ligand (with two carbonyls occupying the bridging sites) was also considered, being less favorable by over 20 kcal/mol (Figure 3, structures **cis-t3e** and **trans-t3e**). This is as expected, since carbyne ligands in polynuclear complexes strongly prefer the bridging

coordination mode rather than the terminal one, due to their strong electron-withdrawing character which exceeds that of carbon monoxide.[38,69] Nevertheless, the exchange of the aminocarbyne group between bridging and terminal positions may be relevant to trans-cis isomerization reactions, reported in the past for complexes of formula $[Fe_2Cp_2(NCS)(CO)(\mu\text{-}CO)\{\mu\text{-}CN(Me)(R)\}]$ (R = Me, Xyl),[70] in alinement with the Adams/Cotton mechanism $[Fe_2Cp_2(CO)_4]$.[71]

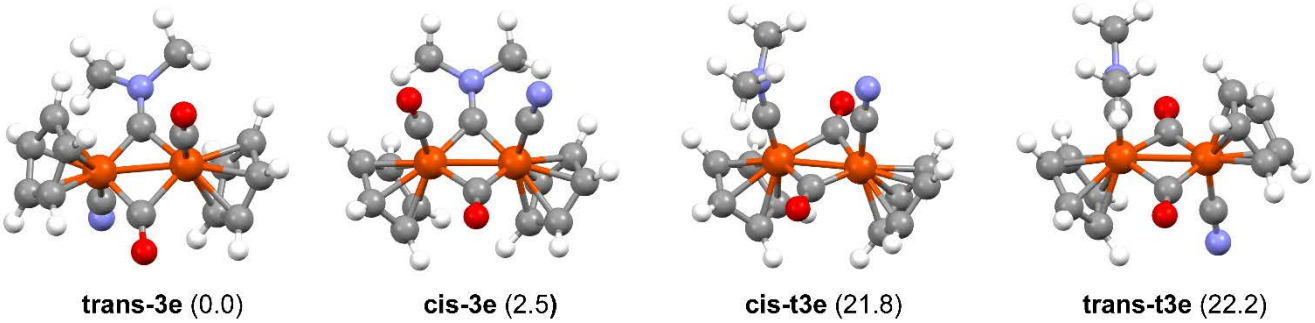

Figure 3. DFT-optimized structures of possible isomers of **3e**, and relative Gibbs energy values. From left to right: cis and trans isomers with bridging-aminocarbyne and cis and trans isomers with terminal-aminocarbyne.

In principle, isopropanol might transfer two hydrogens in a concerted way to **cis-3e** taking advantage of the carbyne-nitrogen bond pair; more precisely, the carbyne carbon is a possible target for a hydride unit,[41,72] while the alcoholic proton could attack the nitrogen. Notwithstanding, this situation would push the $\{NMe_2\}$ group between the Cp rings, leading to a very congested conformation. The same concerted H_2 addition to **trans-3e** (i.e., the most abundant metal species in solution) affording **trans-3eH$_2$**, is still unlikely ($\Delta H^{\ddagger}$ = 44.4 kcal/mol, TS1c as transition state, Figure S17).

Due to the presence in solution of a strong base such as KOH, a fraction of isopropanol is assumed to be deprotonated to give the isopropoxide anion.[73] Isopropoxide is able to interact *via* hydrogen bond with **trans-3e** (reaction complex, **RC**, se Figure 4) and then to donate a hydride to the carbyne carbon (isopropoxide to acetone conversion). The related transition state **TS1** is accessible under the experimental conditions ($\Delta H^{\ddagger}$ = 20.6 kcal/mol, $\Delta G^{\ddagger}$ = 28.8 kcal/mol), and the anionic intermediate adduct **trans-3eH**/acetone consequently forms (**trans-Int1**, ΔH = -13.5 kcal/mol, Figure 4). This

finding reflects the tendency of cationic diiron aminocarbyne complexes of types [**1a-d**]$^{+}$ to undergo hydride addition (usually, from sodium borohydride) at the carbyne carbon.[41,72]

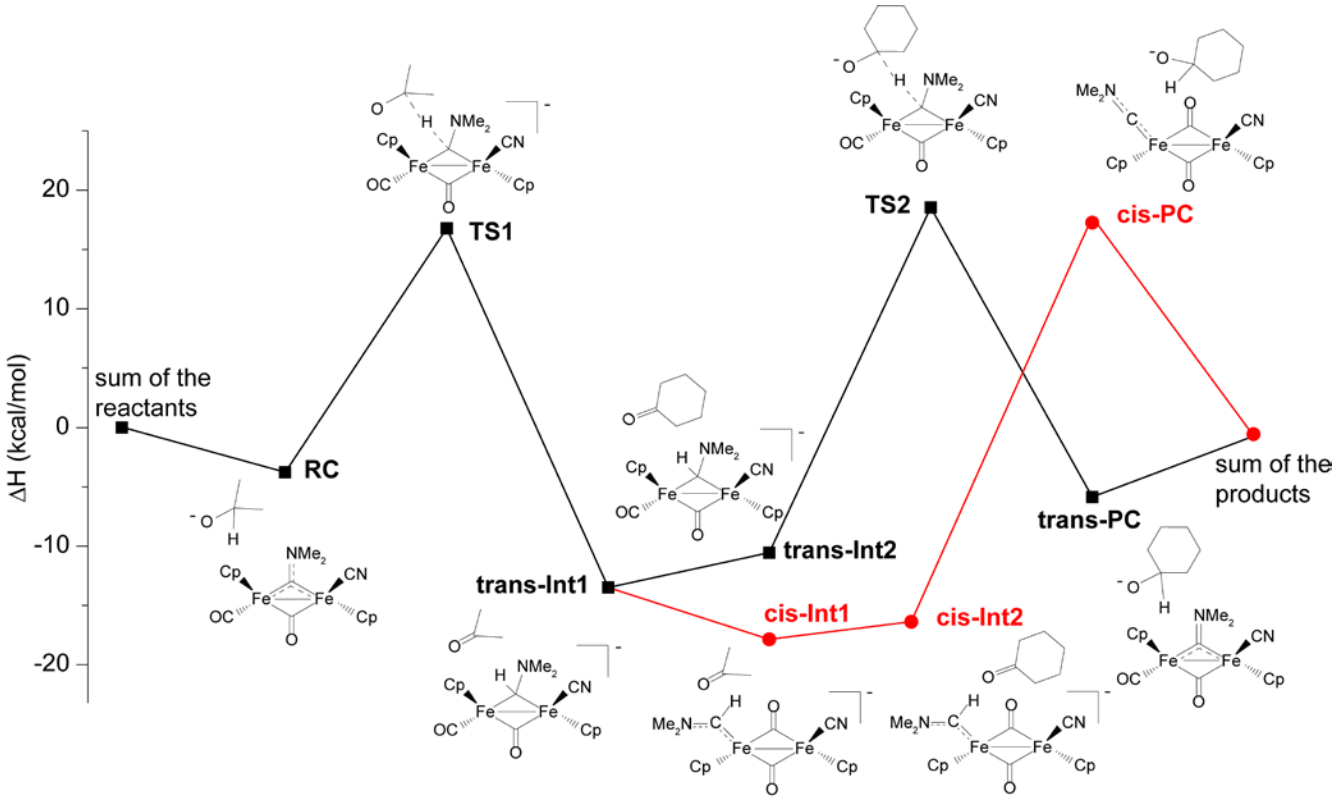

Figure 4. Energy profiles of two reaction paths for TH of cyclohexanone, via initial hydride transfer to the carbyne. **RC** = **trans-3e**/isopropoxide; **trans-Int1** = [**trans-3eH**]$^{-}$/acetone; **cis-Int1** = [**cis-t3eH**]$^{-}$/acetone; **trans-Int2** = [**trans-3eH**]$^{-}$/cyclohexanone; **cis-Int2** = [**cis-t3eH**]$^{-}$/cyclohexanone; **trans-PC** = **trans-3e**/cyclohexanoxide; **cis-PC** = **cis-t3e**/cyclohexanoxide.

The protonation of the amine group belonging to the anion [**trans-3eH**]$^{-}$ by H_2O (generated from hydroxide and isopropanol) would give the neutral **trans-3eH$_2$**. However, this reaction is not thermodynamically feasible, as OH^{-} is a stronger base than [**trans-3eH**]$^{-}$. In this case, **trans-3eH$_2$** should then donate the two protons to cyclohexanone in a concerted way (**TS2c**), but the related activation barrier ($\Delta H^{\ddagger}$ = 39.5 kcal/mol) is too high for the experimental conditions (Figure S17).

From the calculated results, it is possible that [**trans-3eH**]$^{-}$ forms an adduct with cyclohexanone (**trans-Int2** in Figure 4) and subsequently transfers the hydride to the ketone (**TS2**, $\Delta H^{\ddagger}$ = 18.6 kcal/mol). The resulting species may be viewed as the adduct between cyclohexanone and the initial

trans-3e (product complex, **trans-PC**). Due to the stability of [**trans-3eH**]$^-$, the activation enthalpy is quite high (29.1 kcal/mol), justifying the high temperature required for the experiment. We hypothesize that cyclohexanone finally converts into cyclohexanol by capturing a proton from the medium (e.g., water) or during the workup. The overall pathway (Figure 4, black path) would explain why all the different diiron aminocarbyne catalysts are more or less efficient in the TH of cyclohexanone.

The conformational flexibility of the diiron complexes can open up to a second possibility, which is depicted in Figure S17: the isomerization of **trans-3e** to **cis-t3e** would enable the acceptance of two hydrogens from isopropanol, the latter concerted reaction occurring with a high activation enthalpy (**TS3c**, $\Delta H^{\ddagger}$ = 48.8 kcal/mol, Figure S18).

On the other hand, once the aminocarbene species [**trans-3eH**]$^-$ is formed (Figure 4), it can isomerize to [**cis-t3eH**]$^-$, which is 4.2 kcal/mol more stable and comprises the aminoalkylidene ligand {=CHNMe$_2$} in the terminal position, giving the adduct **cis-Int1** with acetone (Figure 4, red path). The preferential occupancy of terminal sites by aminoalkylidene ligands in diiron bis-cyclopentadienyl complexes was previously established.[55,74] A hydride might then migrate from [**cis-t3eH**]$^-$ to the cyclohexanone (a suitable TS has not been found), giving the complex **cis-t3e**/cyclohexanoxide (**cis-PC**, ΔH = 17.8 kcal/mol), see red path in Figure 4. This can return to its more stable isomer, **trans-3e**, and cyclohexanone (ΔH = -0.7 kcal/mol). The activation enthalpy is at least 34.1 kcal/mol (the difference between **cis-PC** and **cis-Int2**, Figure 4), larger than in the case of **trans-Fe$_2$CN** (29.1 kcal/mol).

The protonation of the cyano group in [**cis-t3eH**]$^-$, giving **cis-t3eH$_2$**, shows a prohibitive activation enthalpy (40.2 kcal/mol).

On considering the experimental evidence whereby diiron μ-hydride complexes are probably implicated in the TH reaction catalyzed by [**1a-d**]CF_3SO_3, **2a-c** and **4a** (see above), we extended the DFT study to the model complex [$Fe_2Cp_2(CO)_2$(μ-H){μ-$CNMe_2$}], **2e**. Calculations strongly suggest

that the hydride ligand in **2e** is not reactive toward the cyclohexanone. In any case, as the aminocarbyne moiety is still available, a path analogous to that described above for **trans-3e** (Figure 4, black path) can be computed for **trans-2e**. The activation barrier (21.7 kcal/mol) is slightly higher than that obtained for **cis-3e** (20.6 kcal/mol), but still accessible under the employed experimental conditions. Therefore, the major activity of cyanide complexes appears related to their higher stability under the process conditions.

Overall, DFT outcomes indicate that ketone hydrogenation via hydrogen transfer from isopropanol is viable as catalyzed by aminocarbyne diiron complexes in association with a suitable base, proceeding through the fundamental mediation of the carbyne centre acting as a hydride transferor. This ligand-based mechanism is favored by the coordinative saturation of the metal centers with firmly bound ligands but, on the other hand, takes advantage of the versatility of the diiron framework allowing facile interchange of ligands between terminal and bridging positions and cis and trans configurations, respectively.

To the best of our knowledge, the involvement of alkylidyne (carbyne) ligands in any catalytic cycle of a *chemical* hydrogenation reaction promoted by transition metal complexes is unprecedented. Terminal alkylidyne ligands may be unstable under hydrogenation conditions, and for instance complete dissociation was reported in the case of a mononuclear osmium arene complex.[75] On the other hand, silica-grafted dinuclear niobium and tantalum compounds with a bridging alkylydine ligand were reported to promote the H_2 hydrogenation of aromatic substrates but its role in the catalytic cycle is unlikely.[76]

It should be mentioned that **3e** was previously found to be effective in the electrochemically-induced H_2 production from acetic acid, and in such case the action of the cyanide ligand as a proton abstractor is complementary to that of the aminocarbyne as hydride acceptor.

Conclusions

The conversion of ketones into alcohols via transfer hydrogenation (TH) is a reaction of considerable impact, and the urgency for sustainability to develop efficient catalytic systems based on nonprecious metals goes hand in hand with the exploration of novel mechanistic patterns. Here, we have given the first study assessing the potential of diiron complexes in promoting the TH of ketones from isopropanol. More specifically, a series of easily available diiron complexes, based on the $\{Fe_2Cp_2(CO)_2\}$ frame and containing a bridging aminocarbyne ligand, was screened and revealed a potential to act as TH catalysts in the presence of hydroxide. Neutral compounds with a terminal CN ligand performed better, thus outlining an intriguing structural parallelism with the active site of [FeFe] hydrogenase enzymes.[77] Infrared spectroscopy experiments revealed stability of the diiron-cyanide-aminocarbyne assembly, and suggested that no hydride species is produced during the catalytic cycle. According to DFT calculations, the aminocarbyne ligand acts as a hydride transferor between the hydrogen donor and the ketone reagent. The unique characteristics of the aminocarbyne ligand preserve the carbyne carbon towards alcohol/alkoxide addition while, conversely, non-substituted carbyne ligands[78,79] and thio-carbyne ligands,[80,81] in homologous diiron complexes, manifest a significantly higher electrophilicity. Although the preliminary results reported herein indicate a moderate activity compared to the literature library concerning iron compounds, our work proposes a novel mechanistic possibility for TH reactions (carbyne-centered outer sphere mechanism). A modulation of steric and electronic factors (i.e., aminocarbyne substituents, terminal ligands, Cp substitution), and eventually structural features (introduction of chiral functions for asymmetric hydrogenation) would deserve further investigation pointing to optimal catalytic systems.

Experimental

Materials and methods. Reactants and solvents were purchased from Alfa Aesar, Merck, Strem or TCI Chemicals, and were of the highest purity available. Complexes **[1a]CF_3SO_3**, **[1b]CF_3SO_3**, **[1c]CF_3SO_3** and **[1d]CF_3SO_3**, **2c** and **3c**, **3d** and **4** were prepared according to the respective literature procedures. Syntheses were conducted under N_2 atmosphere using standard Schlenk techniques, and products were conserved under N_2 atmosphere once isolated. Dichloromethane, tetrahydrofuran, and diethyl ether were dried with the solvent purification system mBraun MB SPS5, while acetonitrile was distilled from CaH_2. Chromatography separations were carried out on columns of deactivated alumina (Merck, 4% *w/w* water) using unpurified solvents. IR

spectra of solutions were recorded using a CaF_2 liquid transmission cell (2300-1500 cm^{-1}) on a Perkin Elmer Spectrum 100 FT-IR spectrometer. IR spectra were processed with Spectragryph software.[82] NMR spectra were recorded at 298 K on a Jeol JNM-ECZ500R instrument equipped with a Royal HFX Broadband probe. Chemical shifts (expressed in parts per million) are referenced to the residual solvent peaks.[83] NMR spectra were assigned with the assistance of ^{1}H-^{13}C (*gs*-HSQC and *gs*-HMBC) correlation experiments.[84] NMR signals due to secondary isomeric forms (where it has been possible to detect them) are italicized. Elemental analyses were performed on a Vario MICRO cube instrument (Elementar). Mass spectrometry measurements in positive ion scan mode were performed on samples dissolved in MeOH with an API 4000 instrument (SCIEX) equipped with an Ionspray/APCI source.

Synthesis of $[Fe_2Cp_2(\mu\text{-}H)(CO)_2\{\mu\text{-}CN(Me)(R)\}]$ (R = 4-C_6H_4OMe, 2a; R = Cy, 2b).

$[Fe_2Cp_2(\mu\text{-}H)(CO)_2\{\mu\text{-}CN(Me)(4\text{-}C_6H_4OMe)\}]$, 2a (Figure 5).

Figure 5. Structure of **2a**.

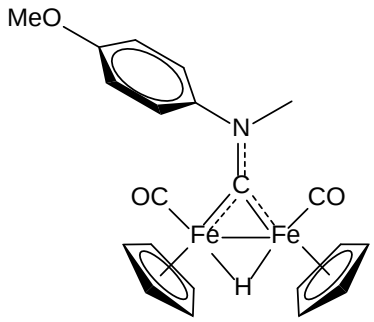

A mixture of **[1a]CF_3SO_3** (128 mg, 0.204 mmol) and Me_3NO (19 mg, 0.25 mmol) in MeCN (10 mL) was stirred for ca. 1 hour, conversion of **[1a]$^+$** into $[Fe_2Cp_2(CO)(\mu\text{-}CO)(NCMe)\{\mu\text{-}CN(Me)(4\text{-}C_6H_4OMe)\}]CF_3SO_3$ being monitored by IR spectroscopy. After complete consumption, $NaBH_4$ (24 mg, 0.63 mmol) was added to the mixture and then stirred for a further 2 h. After removal of volatiles, the mixture was redissolved in Et_2O (15 mL) and filtered through celite. After removal of Et_2O and extensive drying, a dark-red powder was isolated. Yield 54 mg (59%). Anal. calcd. for $C_{21}H_{21}Fe_2NO_3$: C, 56.41; H, 4.73; N, 3.13. Found: C, 56.48; H, 4.68; N, 3.20. IR (CH_3CN): $\tilde{\nu}/cm^{-1}$ = 1936s (CO), 1892m (CO). IR (CH_2Cl_2): $\tilde{\nu}/cm^{-1}$ = 1939s (CO), 1897m (CO). ^1H NMR ($CDCl_3$):

δ/ppm = 7.42-6.53 (m, arom); 4.41, 4.36 (s, Cp); 3.83, 3.66 (s, OMe + NMe); −17.84 (s, μ-H). ^{1}H NMR spectrum unclean due to incipient decomposition, only assignments for the prevalent isomeric form are given.

$[Fe_2Cp_2(\mu\text{-}H)(CO)_2\{\mu\text{-}CN(Me)(Cy)\}]$, 2b (Figure 6).

Figure 6. Structure of **2b**.

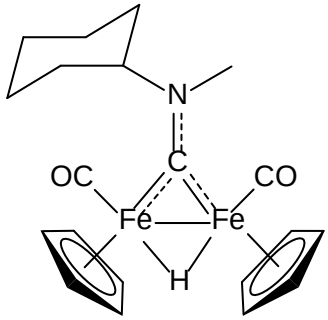

The title compound was prepared by the same procedure described for **2a**, from **$[1b]CF_3SO_3$** (117 mg, 0.195 mmol), Me_3NO (23 mg, 0.31 mmol) and $NaBH_4$ (22 mg, 0.58 mmol). Dark-red powder, yield 51 mg (62%). Anal. calcd. for $C_{20}H_{25}Fe_2NO_2$: C, 56.77; H, 5.95; N, 3.31. Found: C, 56.71; H, 6.05; N, 3.25. IR (CH_3CN): ũ/cm^{-1} = 1933s (CO), 1890m (CO). IR (CH_2Cl_2): ũ/cm^{-1} = 1938s (CO), 1895m (CO). ^{1}H NMR ($CDCl_3$): δ/ppm = 5.50 (m, 1 H, CH^{Cy}); 4.89 (s, 3 H, NMe); 4.88, 4.19 (s, 10 H, Cp); 2.45, 2.28, 1.91-1.72, 1.59 (m, 10 H, $CH_2{}^{Cy}$); −17.45 (s, μ-H). ^{1}H NMR spectrum unclean due to incipient decomposition, only assignments for the prevalent isomeric form are given.

Synthesis and characterization of $[Fe_2Cp_2(CN)(CO)(\mu\text{-}CO)\{\mu\text{-}CN(Me)(R)\}]$ (R = 4-C_6H_4OMe, 3a; R = Cy, 3b).

$[Fe_2Cp_2(CN)(CO)(\mu\text{-}CO)\{\mu\text{-}CN(Me)(4\text{-}C_6H_4OMe)\}]$, 3a (Figure 7).

Figure 7. Structure of **3a**.

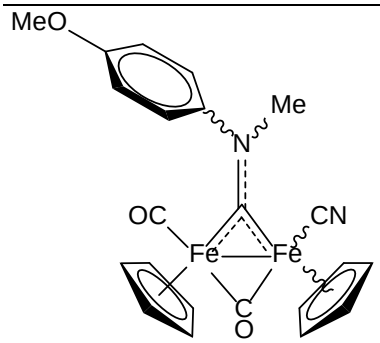

A solution of [**1a**]CF_3SO_3 (131 mg, 0.210 mmol) in MeCN (10 mL) was treated with Me_3NO (21 mg, 0.28 mmol) to obtain the acetonitrile adduct as described above for the synthesis of **2a**. Volatiles were removed under vacuum, and the dark-brown residue was dissolved in dichloromethane (5 mL). Tetrabutylammonium cyanide (57 mg, 0.21 mmol) was added to this solution, and the resulting mixture was stirred for 1 hour at room temperature. The final solution was charged on top of an alumina column. Impurities were separated using CH_2Cl_2 and CH_2Cl_2/THF (4/1 v/v) as eluent, then a green fraction corresponding to **3a** was collected with THF. Solvent was removed under reduced pressure, and the residue was suspended in hexane for 24 hours. After filtration, the solid was dried under vacuum. Green powder, yield 68 mg (68%). Anal. calcd. for $C_{22}H_{20}Fe_2N_2O_3$: C, 55.97; H, 4.27; N, 5.93. Found: C, 55.90; H, 4.21; N, 6.03. IR (CH_2Cl_2): $\tilde{\upsilon}$/cm^{-1} = 2091w (C≡N), 1979s (CO), 1963s (CO), 1804vs (μ-CO), 1587vw (μ-CN). ^{1}H NMR ($CDCl_3$): δ/ppm = 7.85- 7.43, 7.04-6.90 (m, 4 H, C_6H_4); *4.94*, 4.88, 4.82, *4.76,* 4.33, *4.30*, 4.24, *4.17* (s, 10 H, Cp); *4.67, 4.56,* 4.52, 4.42 (s, 3 H, NMe); *3.89*, 3.87, 3.86, *3.81* (s, 3 H, OMe). $^{13}C\{^1H\}$ NMR ($CDCl_3$): δ/ppm = 335.9 (μ-CN); 263.6 (μ-CO); 212.4 (CO); 159.2, 159.1, 144.4, 143.7, 127.2, 126.7, 126.4, 115.0, 114.8, 114.7 (C_6H_4); 122.6, *119.4* (C≡N); 90.2, 90.1, 89.4, 89.0, 87.4, 87.1, 86.9, 86.9 (Cp); 55.8 (NMe); 55.7, 55.0 (OMe). Isomer ratio: 35:21:27:17. ESI-MS(+): $[M]^+$ *m/z* = 473.09 (theoretical for $[C_{22}H_{20}Fe_2N_2O_3]^+$: *m/z* = 473.02).

[Fe_2Cp_2(CN)(CO)(μ-CO){μ-CN(Me)(Cy)}], 3b (Figure 8).

Figure 8. Structure of **3b**.

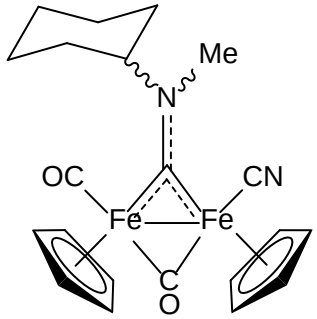

The title compound was prepared by the same procedure described for **3a**, from [**1b**]CF_3SO_3 (116 mg, 0.194 mmol), Me_3NO (23 mg, 0.31 mmol) and NBu_4CN (52 mg, 0.19 mmol). Green powder, yield 61 mg (70%). Anal. calcd. for $C_{21}H_{24}Fe_2N_2O_2$: C, 56.29; H, 5.40; N, 6.25. Found: C, 56.20; H, 5.32; N, 6.33. IR (CH_2Cl_2): $\tilde{\upsilon}/cm^{-1}$ = 2091vw (C≡N), 1978vs (CO), 1801s (μ-CO), 1560w (μ-CN). ^1H NMR ($CDCl_3$): δ/ppm = 4.82, 4.79, 4.76, 4.72 (s, 10 H, Cp); 4.64 (m, 1H, CH^{Cy}); 4.06, *3.92* (s, 3 H, NMe); 2.30, 2.11-1.59 (m, 10 H, $CH_2{}^{Cy}$). $^{13}C\{^1H\}$ NMR ($CDCl_3$): δ/ppm = *327.8*, 327.6 (μ-CN); *263.5*, 263.4 (μ-CO); 212.5, *212.2* (CO); 122.5, *119.4* (C≡N); 87.1, *87.0, 86.8*, 86.6 (Cp); 75.8, *75.3* (CH^{Cy}); 44.5, *44.1* (NMe); 34.2, 31.8, 31.7, 31.6, 31.4, 26.1, 25.9, 25.8, 25.4, 25.3 ($CH_2{}^{Cy}$). Isomer ratio= 71:29. ESI-MS(+): $[M]^+$ *m/z* = 449.11 (theoretical for $[C_{21}H_{24}Fe_2N_2O_2]^+$: *m/z* = 449.06).

Synthesis and characterization of $[Fe_2Cp_2(Cl)(CO)(\mu\text{-}CO)\{\mu\text{-}CN(Me)(4\text{-}C_6H_4OMe)\}]$, 4a.

$[Fe_2Cp_2(Cl)(CO)(\mu\text{-}CO)\{\mu\text{-}CN(Me)(C_6H_4(4\text{-}OMe))\}]$, 4a (Figure 9).

Figure 9. Structure of **4a**.

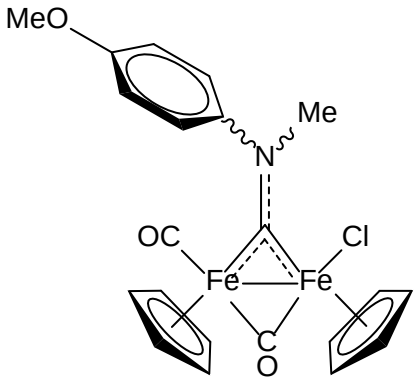

A solution of [**1a**]CF_3SO_3 (136 mg, 0.218 mmol) in MeCN (10 mL) was treated with Me_3NO (30 mg, 0.27 mmol) to obtain the acetonitrile adduct as described above for the synthesis of **2a**. Volatiles were removed under

vacuum to afford a dark-brown residue which was dissolved in THF (5 mL). Lithium chloride (42 mg, 0.99 mmol) was added to this solution, and the mixture was stirred for 3 h at room temperature. The final mixture was charged on top of an alumina column, and a brown fraction corresponding to **4a** was collected using THF as eluent. Solvent was removed under reduced pressure and the residue was suspended in pentane for 24 hours. After filtration, the solid was dried under vacuum. Brown powder, yield 76 mg (72%). Anal. calcd. for $C_{21}H_{20}ClFe_2NO_3$: C, 52.38; H, 4.19; N, 2.91. Found: C, 52.43; H, 4.21; N, 2.99. IR (CH_2Cl_2): ũ/cm^{-1} = 1979vs (CO), 1800s (μ-CO), 1587w (μ-CN). ^{1}H NMR ($CDCl_3$): δ/ppm = 7.94, 7.91, 7.51, 7.49, 7.11, 7.08, 7.06 (C_6H_4); 4.98, *4.58* (NMe); *4.79*, 4.71, 4.26, *4.15* (Cp); *3.91*, 3.90 (OMe). $^{13}C\{^1H\}$ NMR ($CDCl_3$): δ/ppm = 342.7, *342.6* (μ-CN); 267.4 (μ-CO); 212.9, *212.2* (CO); *159.3*, 159.1, 144.6, *144.0*, *127.3*, 126.8, 115.0, *114.6* (C_6H_4); *89.6*, *88.3*, 87.0, 86.9 (Cp); 55.8 (NMe); 55.7, *54.7* (OMe). Isomer ratio: 2:1. Crystals suitable for X-ray analysis were obtained from slow diffusion of pentane into a solution of **4a** in dichloromethane at -30 °C. ESI-MS(+): $[M - Cl]^+$ *m/z* = 446.10 (theoretical for $[C_{21}H_{20}Fe_2NO_3]^+$: *m/z* = 449.08).

X-ray crystallography

Crystal data and collection details for **4a** are reported in Table 5. Data were recorded on a Bruker APEX II diffractometer equipped with a PHOTON2 detector using Mo–Kα radiation. The structure was solved by direct methods and refined by full-matrix least-squares based on all data using F^2.[85] Hydrogen atoms were fixed at calculated positions and refined using a riding model.

Table 5. Crystal data and measurement details for **4a**.

	4a
Formula	$C_{21}H_{20}ClFe_2NO_3$
FW	481.53
T, K	100(2)
λ, Å	0.71073
Crystal system	Monoclinic
Space group	$P2_1/c$
a, Å	17.6169(17)
b, Å	6.7690(6)

c, Å	17.0565(16)
β, °	108.787(3)
Cell Volume, Å^3	1925.9(3)
Z	4
D_c, g·cm^{-3}	1.661
μ, mm^{-1}	1.668
F(000)	984
Crystal size, mm	0.21×0.19×0.12
θ limits,°	2.423-27.000
Reflections collected	24884
Independent reflections	4194 [R_{int} = 0.0746]
Data / restraints /parameters	4194 / 150 / 230
Goodness on fit on F^2	1.234
R_1 ($I > 2\sigma(I)$)	0.1050
wR_2 (all data)	0.2613
Largest diff. peak and hole, e Å^{-3}	1.957 / –1.044

Catalytic studies

General procedure. The selected catalyst and the base, dissolved in isopropanol (2 mL), were added to a Schlenk tube under N_2 atmosphere. The ketone reagent (ca. 1 mmol) was added, and the mixture was heated at reflux for a variable time. At the end of the reaction, the system was cooled to room temperature; an aliquot of the solution (ca. 0.2 mL) was transferred into an NMR tube and mixed with 0.5 mL of $CDCl_3$. Ketone to alcohol conversion was determined by means of ^{1}H NMR spectroscopy.

Stability studies

The selected complex (0.050 mmol) and KOH (10 mg, 0.178 mmol) were placed in a 15 mL Schlenck tube, that was evacuated and filled with dinitrogen. The vacuum/N_2 cycle was repeated twice. Isopropanol (5 mL) was added, and the resulting mixture was heated at reflux temperature. After 1 hour, an aliquot of the solution (ca 0.5 mL) was dried, the residue was dissolved in dichloromethane and this new solution was controlled by IR spectroscopy. The same procedure was repeated after 2 h and 10 h, and only for **3a** after 24 h and 3 days. The identity of **2a**, as formed from **[1a]CF_3SO_3** and **4a**, was confirmed by ^{1}H NMR analyses on $CDCl_3$ solutions of the

residues obtained from ca. 1 mL aliquots of the respective reaction solutions which were dried under vacuum (t = 1 h).

From [1a]CF_3SO_3. IR (CH_2Cl_2, t_0): ũ/cm^{-1} = 2022vs (CO), 1990w (CO), 1836s (μ-CO), 1606w, 1563w, 1540w (μ-CN), 1507w. IR (CH_2Cl_2, 1 h): ũ/cm^{-1} = 2021vs (CO), 1989w (CO), 1965s, 1940s (CO, **2a**), 1897w (CO, **2a**), 1836m (μ-CO), 1789br, 1673s, 1514vs. ^{1}H NMR ($CDCl_3$, 1 h): δ/ppm = -16.77 (br, μ-H). Complete degradation at t = 10 h.

From 3a. IR (CH_2Cl_2, t_0): ũ/cm^{-1} = 2091w (C≡N), 1979s (CO), 1963s (CO), 1804vs (μ-CO), 1587vw (μ-CN). IR (CH_2Cl_2, 1 h): ũ/cm^{-1} = 2091w (C≡N), 1979w (CO), 1963vs (CO), 1804s (μ-CO). IR (CH_2Cl_2, t2 h, unchanged at t = 24 h): ũ/cm^{-1} = 2091w (C≡N), 1963vs (CO), 1804s (μ-CO). Complete degradation at t = 3 d.

From 4a. IR (CH_2Cl_2, t_0): ũ/cm^{-1} = 1979vs (CO), 1800s (μ-CO), 1598w (μ-CN). IR (CH_2Cl_2, 1 h): ũ/cm^{-1} = 1979w (CO), 1937s (CO, **2a**), 1898m (CO, **2a**), 1800br (μ-CO). Complete degradation at t = 10 hours.

DFT calculations

All geometries were optimized with ORCA 4.2.0,[86] using the B97 functional in conjunction with a triple-ζ quality basis set (def2-TZVP). The dispersion corrections were introduced using the Grimme D3-parametrized correction and the Becke Johnson damping to the DFT energy.[87] All the structures were confirmed to have no imaginary frequencies (intermediate species) or only one (transition states). The solvent was considered through the continuum-like polarizable continuum model (C-PCM, isopropanol).

Author contribution

G.B.: synthesis and spectroscopic characterization of complexes; L.B.: assitance with synthesis/characterization; S.Z.: X-ray diffraction analysis; G.P.: funding; G.C.: DFT calculations and writing; F.M.: supervision, writing and funding.

Acknowledgements

We thank the University of Pisa for financial support (Fondi di Ateneo 2021). Dr. Andrea Raffaelli (University of Pisa) is gratefully acknowledged for ESI-MS analyses.

Supporting Information Available

NMR and IR spectra of diiron complexes; DFT data. CCDC reference number 2190681 (**4a**) contains the supplementary crystallographic data for the X-ray study reported in this work. This data is available free of charge at http://www.ccdc.cam.ac.uk/structures.

References

1 X. Zhang, P.-L. Shao, Industrial Applications of Asymmetric (Transfer) Hydrogenation, in Asymmetric Hydrogenation and Transfer Hydrogenation, V. Ratovelomanana-Vidal, P. Phansavath, Eds., Wiley-VCH, **2021**, pp. 175-219.

2 C. Pettinari, F. Marchetti, D. Martini, Metal Complexes as Hydrogenation Catalysts, in Comprehensive Coordination Chemistry II, J. A. McCleverty, T. J. Meyer, Eds., Elsevier, Vol. 9, **2004**, pp 75-139.

3 W. S. Knowles, R. Noyori, *Acc. Chem. Res.* **2007**, *40*, 1238.

4 P. Kumar, R. K. Gupta, D. Shankar Pandey, *Chem. Soc. Rev*. **2014**, *43*, 707.

5 W. Wu, T. Seki, K. L. Walker, R. M. Waymouth, *Organometallics* **2018**, *37*, 1428.

6 A. E. Clapham, A. Hadzovic, R. H. Morris, *Coord. Chem. Rev.* **2004**, *248*, 2201.

7 J. S. M. Samec, J. E. Bäckvall, *Chem. Eur. J.* **2002**, *8*, 2955.

8 H.-J. Pan, Y. Zhang, C. Shan, Z. Yu, Y. Lan, Y. Zhao, *Angew. Chem. Int. Ed.* **2016**, *55*, 9615.

9 Y. Wang, Z. Huang, X. Leng, H. Zhu, G. Liu, Z. Huang, *J. Am. Chem. Soc.* **2018**, *140*, 4417.

10 C. Michon, K. MacIntyre, Y. Corre, F. Agbossou-Niedercorn, *ChemCatChem* **2016**, *8*, 1755.

11 D. Wang, D. Astruc, *Chem. Rev.* **2015**, *115*, 6621.

12 D. Baidilov, D. Hayrapetyan, A. Y. Khalimon, *Tetrahedron* **2021**, *98*, 132435.

13 Y.-Y. Li, S.-L. Yu, W.-Y. Shen, J.-X. Gao, *Acc. Chem. Res.* **2015**, *48*, 2587.

14 B. N. Bhawal, B. Morandi, *ACS Catal.* **2016**, *6*, 7528−7535.

15 Hydrogenation with Low Cost Transition Metals, **2016**, J. Sa, A. Srebowata (Eds.), CRC Press, Boca Raton (FL, USA).

16 M. K. Whittlesey, in Science of Synthesis: N-Heterocyclic Carbenes in Catalytic Organic Synthesis, S. P. Nolan, C. S. J. Cazin, eds., **2017**, Vol. 1, pp. 285-300.

17 G. Bresciani, S. Zacchini, F. Marchetti, G. Pampaloni, *Dalton Trans.* **2021**, *50*, 5351.

18 S. Rana, J. P. Biswas, S. Paul, A. Paik, D. Maiti, *Chem. Soc. Rev.* **2021**, *50*, 243-472.

19 I. Bauer, H.-J. Knölker, Iron Complexes in Organic Chemistry in Iron Catalysis in Organic Chemistry: Reactions and Applications, B. Plietker, Ed., **2008**, Wiley-VCH, Weinheim, pp. 1-28.

20 S. Enthaler, Iron complexes as substitutes for toxic metals in asymmetric synthesis, in Comprehensive Inorganic Chemistry II, J. Reedijk, K. Poeppelmeier, Eds., **2013**, Vol. 6, pp. 549-562.

21 D. Wei, C. Darcel, *Chem. Rev.* **2019**, *119*, 2550.

22 D. E. Prokopchuk, S. A. M. Smith, R. H. Morris, Ligands for Iron-based Homogeneous Catalysts for the Asymmetric Hydrogenation of Ketones and Imines, in Ligand Design in Metal Chemistry: Reactivity and Catalysis, M. Stradiotto, R.J. Lundgren, Eds., Chapter 8, Wiley, Weinheim, **2016**, pp. 205–236.

23 Y. Li, S. Yu, X. Wu, J. Xiao, W. Shen, Z. Dong, J. Gao, *J. Am. Chem. Soc.* **2014**, *136*, 4031.

24 C. Malchau, T. Milbert, T. R. Eger, D. V. Fries, P. J. Pape, B. Oelkers, Y. Sun, S. Becker, M. H. Prosenc, G. Niedner-Schatteburg, W. R. Thiel, *Chem. Eur. J.* **2021**, *27*, 15209.

25 P. Das, T. Elder, W. W. Brennessel, S. C. Chmely, *RSC Adv.* **2016**, *6*, 88050.

26 M. D. Bala, M. I. Ikhile, *J. Mol. Catal. A* **2014**, *385*, 98.

27 M. Kamitani, Y. Nishiguchi, R. Tada, M. Itazaki, H. Nakazawa, *Organometallics* **2014**, *33*, 1532.

28 V. V. Kandepi, M. Krishna, J. M. S. Cardoso, E. Peris, B. Royo, *Organometallics* **2010**, *29*, 2777.

29 T. W. Funk, A. R. Mahoney, R. A. Sponenburg, K. P. Zimmerman, D. K. Kim, E. E. Harrison, *Organometallics* **2018**, *37*, 1133.

30 C. Sui-Seng, F. Freutel, A. J. Lough, R. H. Morris, *Angew. Chem. Int. Ed.* **2008**, *47*, 940.

31 R. H. Morris, *Dalton Trans.* **2018**, *47*, 10809.

32 S. A. Moyer, T. W. Funk, *Tetrahedron Lett.* **2010**, *51*, 5430.

33 V. Ritleng, M. J. Chetcuti, *Chem. Rev.* **2007**, *107*, 797.

34 C. B. van Beek, N. P. van Leest, M. Lutz, S. D. de Vos, R. J. M. Klein Gebbink, B. de Bruin, D. L. J. Broere, *Chem. Sci.* **2022**, *13*, 2094.

35 H. Land, M. Senger, G. Berggren, S. Stripp, *ACS Catal.* **2020**, *10*, 7069.

36 J. T. Kleinhaus, F. Wittkamp, S. Yadav, D. Siegmund, U.-P. Apfel, *Chem. Soc. Rev.* **2021**, *50*, 1668.

37 R. Mazzoni, M. Salmi, V. Zanotti, *Chem. Eur. J.* **2012**, *18*, 10174.

38 L. Biancalana, F. Marchetti, *Coord. Chem. Rev.* **2021**, *449*, 214203.

39 According to IUPAC rules, metal compounds containing a carbyne ligand are named "alkylidyne" complexes regardless of the nature of both the carbyne substituents and the metal fragment. See: Transition Metal Carbyne Complexes, F. R. Kreiβl, Ed., Nato Science Series C, Springer Dordrecht, **1993**. On considering that the term “aminocarbyne”, rather than “aminoalkylidyne”, is largely used in the literature, the former is generally adopted in this article.

40 L. Biancalana, M. De Franco, G. Ciancaleoni, S. Zacchini, G. Pampaloni, V. Gandin, F. Marchetti, *Chem. Eur. J.* **2021**, *27*, 10169.

41 F. Marchetti, *Eur. J. Inorg. Chem.* **2018**, 3987.

42 A. J. L. Pombeiro, *J. Organomet. Chem.* **2005**, *690*, 6021.

43 S. Anderson, A. F. Hill, *Organometallics* **1995**, *14*, 1562.

44 G. Agonigi, M. Bortoluzzi, F. Marchetti, G. Pampaloni, S. Zacchini, V. Zanotti, *Eur. J. Inorg. Chem.* **2018**, 960.

45 S. E. Clapham, A. Hadzovic, R. H. Morris, *Coord. Chem. Rev.* **2004**, *248*, 2201.

46 C. A. Sandoval, F. Bie, A. Matsuoka, Y. Yamaguchi, H. Naka, Y. Li, K. Kato, N. Utsumi, K. Tsutsumi, T. Ohkuma, K. Murata, R. Noyori, *Chem. Asian J.* **2010**, *5*, 806.

47 F. Arrigoni, L. Bertini, L. De Gioia, A. Cingolani, R. Mazzoni, V. Zanotti, G. Zampella, *Inorg. Chem.* **2017**, *56*, 13852.

48 F. Arrigoni, L. Bertini, L. De Gioia, G. Zampella, R. Mazzoni, A. Cingolani, I. Gualandi, D. Tonelli, V. Zanotti, *Inorg. Chim. Acta* **2020**, *510*, 119745.

49 T.-Y. Luh, *Coord. Chem. Rev.* **1984**, *60*, 255.

50 G. Bresciani, L. Biancalana, G. Pampaloni, S. Zacchini, G. Ciancaleoni, F. Marchetti, *Molecules* **2021**, *26*, 7088.

51 V. G. Albano, L. Busetto, M. Monari, V. Zanotti, *J. Organomet. Chem.* **2000**, *606*, 163.

52 A. Widera, E. Kaifer, H. Wadepohl, H.-J. Himmel, *Chem. Eur. J.* **2018**, 1209.

53 J. L. Look, D. D. Wick, J. M. Mayer, K. I. Goldberg, *Inorg. Chem.* **2009**, *48*, 1356.

54 G. Bresciani, S. Schoch, L. Biancalana, S. Zacchini, M. Bortoluzzi, G. Pampaloni, F. Marchetti, *Dalton Trans.* **2022**, *51*, 1936.

55 F. Marchetti, Alkylidyne and Alkylidene Complexes of Iron. In: Parkin, G., Meyer, K., O'Hare, D. (eds.), *Comprehensive Organometallic Chemistry IV*, **2022**, Vol. 7, pp. 210-257 Kidlington, UK: Elsevier. DOI: 10.1016/B978-0-12-820206-7.00105-0.

56 A. J. L. Pombeiro, M. F. C. Guedes da Silva, R. A. Michelin, *Coord. Chem. Rev*. **2001**, 218, 43–74.

57 M. A. Alvarez, M. E. García, D. García-Vivó, E. Huergo, M. A. Ruiz, *J. Organomet. Chem*. **2021**, 936, 121708

58 R. T. Kumah, P. Vijayan, S. O. Ojwach, *Catal. Letters* **2021**, *151*, 344.

59 R. Lopes, Á. Raya-Barón, M. P. Robalo, C. Vinagreiro, S. Barroso, M. J. Romão, I. Fernández, M. M. Pereira, B. Royo, *Eur. J. Inorg. Chem.* **2021**, 22.

60 L. Kathuria, N. U. Din Reshi, A. G. Samuelson, *Chem. Eur. J.* **2020**, *26*, 7622.

61 M. G. Coleman, A. N. Brown, B. A. Bolton, H. Guana, *Adv. Synth. Catal.* **2010**, *352*, 967.

62 S. Yaşar, E. O. Karaca, C. Şahin, I. Özdemir, O. Şahin, O. Büyükgüngör, *J. Organomet. Chem.* **2015**, *789*, 1.

63 M. Bortoluzzi, G. Bresciani, F. Marchetti, G. Pampaloni, S. Zacchini, *Dalton Trans*. **2015**, *44*, 10030.

64 G. Bresciani, M. Bortoluzzi, C. Ghelarducci, F. Marchetti, G. Pampaloni, *New J. Chem.* **2021**, *45*, 4340.

65 M. G. Rhomberg, B. B. Owen, *J. Am. Chem. Soc.* **1951**, *73*, 5904.

66 J. R. Sweet, W. A. G. Graham, *Organometallics* **1982**, *1*, 982.

67 J. C. M. Ritter, R. G. Bergman, *J. Am. Chem. Soc.* **1998**, *120*, 6826.

68 O. Blum, D. Milstein, *J. Organomet. Chem.* **2000**, *593–594*, 479.

69 A. I. F. Venàncio, M. F. C. Guedes da Silva, L. M. D. R. S. Martins, J. J. R. Fraùsto da Silva, A. J. L. Pombeiro, *Organometallics* **2005**, *24*, 4654.

70 L. Busetto, F. Marchetti, S. Zacchini, V. Zanotti, *Inorg. Chim. Acta* **2005**, *358*, 1204.

71 L. J. Farrugia, *J. Chem. Soc. Dalton Trans.* **1997**, 1783.

72 L. Busetto, V. Zanotti, *J. Organomet. Chem.* **2005**, *690*, 5430.

73 G. Bresciani, E. Antico, G. Ciancaleoni, S. Zacchini, G. Pampaloni, F. Marchetti, *ChemSusChem* **2020**, *13*, 5586.

74 V. Zanotti, S. Bordoni, L. Busetto, l. Carlucci, A. Palazzi, R. Serra, V. G. Albano, M. Monari, F. Prestopino, F. Laschi, P. Zanello, *Organometallics* **1995**, *14*, 5232.

75 M. L. Buil, J. J. F. Cardo, M. A. Esteruelas, I. Fernández, E. Oñate, *Organometallics* **2015**, *34*, 547.

76 R. D. Profilet, A. P. Rothwell, I. P. Rothwell, *J. Chem. Soc., Chem. Commun.* **1993**, 42.

77 W. Lubitz, H. Ogata, O. Rüdiger, E. Reijerse, *Chem. Rev.* **2014**, *114*, 4081.

78 C. P. Casey, M. W. Meszaros, S. R. Marder, P. J. Fagant, *J. Am. Chem. Soc.* **1984**, *106*, 3680.

79 C. P. Casey, M. Crocker, G. P. Niccolai, P. J. Fagan, M. S. Konings, *J. Am. Chem. Soc.* **1988**, *110*, 6070.

80 L. Busetto, V. Zanotti, L. Norfo, A. Palazzi, V. G. Albano, D. Braga, *Organometallics* **1993**, *12*, 190.

81 L. Busetto, V. Zanotti, *Inorg. Chim. Acta* **2008**, *361*, 3004.

82 F. Menges, "Spectragryph - optical spectroscopy software", Version 1.2.5, @ **2016-2017**, http://www.effemm2.de/spectragryph.

83 G. R. Fulmer, A. J. M. Miller, N. H. Sherden, H. E. Gottlieb, A. Nudelman, B. M. Stoltz, J. E. Bercaw, K. I. Goldberg, *Organometallics* **2010**, *29*, 2176.

84 W. Willker, D. Leibfritz, R. Kerssebaum, W. Bermel, *Magn. Reson. Chem.* **1993**, *31*, 287.

85 G. M. Sheldrick, *Acta Crystallogr. C* **2015**, *71*, 3.

86 F. Neese, *Comput. Mol. Sci.* **2017**, *8*, e1327.

87 S. Grimme, J. Antony, S. Ehrlich, H. Krieg, *J. Chem. Phys.* **2010**, *132*, 154104.